

## Supporting Information

### Platinum(II) complex bearing deprotonated

### 2-(diphenylphosphino)benzoic acid for superior phosphorescence of monomers

Bin Zhang,<sup>a</sup> Lina Zhang,<sup>a,b</sup> Chunmei Liu,<sup>a</sup> Yanyan Zhu,<sup>a</sup> Mingsheng Tang,<sup>a</sup> Chenxia Du<sup>a</sup>  
and Maoping Song<sup>\*a</sup>

#### I. Experimental Section.

**General information and materials.** All commercial chemicals were used without further purification unless otherwise stated. The dry solvents were treated with an appropriate drying reagent and degassed prior to use. Unless otherwise specified, all air and moisture sensitive reactions were carried out under an argon atmosphere. Bubbling the samples with argon prior to emission spectra, quantum yield and lifetime determinations. The iridium dimer  $[(C^{\wedge}N)_2Ir(\mu-Cl)]_2$ <sup>1</sup> and platinum dimer  $[(C^{\wedge}N)Pt(\mu-Cl)]_2$ <sup>2</sup> ( $C^{\wedge}N = ppy$ ) were synthesized according to literature method.

**Physical Measurements.** NMR spectra were obtained by using a Bruker DPX-400MHz spectrometer in DMSO-*d*<sub>6</sub>. Electrospray ionization (ESI) mass spectra were conducted in positive ion mode using a Bruker Esquire 3000 instrument (CH<sub>3</sub>OH was used as solvent). Elemental analysis for C, H, and N were determined with a Carlo-Erba 1106 Elemental Analyzer. Absorption spectra were carried out on a Perkin-Elmer Lambda 900 spectrometer at room temperature. The steady-state emission was performed on a Jobin-Yvon-Horiba FluoroMax-4P spectrometer. The phosphorescent lifetimes of the complexes were obtained using a spectrophotometer from Edinburgh Instruments Ltd (FLS920). Solution quantum efficiency measurements were calculated by a comparison of the emission intensities (integrated areas) of a standard sample (Ir(ppy)<sub>3</sub>,  $\Phi = 0.40$ )<sup>3</sup> and the unknown sample at room temperature in a solution of dichloromethane. The relative method were based on equation  $\Phi_{unk} = \Phi_{std}((\eta_{unk}^2 A_{std} I_{unk}) / (\eta_{std}^2 A_{unk} I_{std}))$ , where the  $\Phi$  denotes the quantum yield,  $\eta$  is the refractive index, A is the absorbance, and I is the integrated area of the emission band, subscript unk is the sample and subscript std is the Ir(ppy)<sub>3</sub> reference.<sup>4</sup> The quantum efficiency of Pt-1 in solid state was obtained through an absolute method by employing

an integrating sphere.

**Synthesis of the Ir-1 Complex.** A mixture of cyclometalated Ir(III)  $\mu$ -chloro-bridged dimer (1.08g, 1.0 mmol), HL<sub>1</sub> (0.76g, 2.5 mmol) and Na<sub>2</sub>CO<sub>3</sub> (1.06g, 10.0 mmol) in 2-ethoxyethanol (50 mL) was refluxed under a argon atmosphere for 16 h. After cooling to room temperature, the solvent was evaporated at low pressure. The obtained crude product was washed by water and then purified by column chromatography on silica gel using CH<sub>2</sub>Cl<sub>2</sub>/EtOAc as the eluent to afford a yellow product with a yield of 43% (0.69 g). <sup>1</sup>H NMR (400 MHz, DMSO-*d*<sub>6</sub>):  $\delta$  8.29 (1H, d), 8.16-8.10 (2H, m), 8.05 (1H, d), 7.84-7.71 (5H, m), 7.52-7.38 (5H, m), 7.34-7.25 (3H, m), 7.06-7.01 (2H, m), 6.93-6.71 (7H, m), 6.52-6.50 (1H, m), 6.39-6.35 (2H, m), 6.78-6.75 (1H, m); <sup>31</sup>P NMR (162 MHz, DMSO-*d*<sub>6</sub>):  $\delta$  -3.03; m/z: [M+1]<sup>+</sup> calc 807.2, found 807.4; Anal. Calcd for C<sub>41</sub>H<sub>30</sub>N<sub>2</sub>O<sub>2</sub>PIr: C, 61.11; H, 3.75; N, 3.48. Found: C, 61.05; H, 3.76; N, 3.46.

**Synthesis of the Pt-1 Complex.** The cyclometalated platinum dimer (1.23 g, 1.6 mmol) reacted with HL<sub>1</sub> (0.98 g, 3.2 mmol) and Na<sub>2</sub>CO<sub>3</sub> (1.69 g, 15.9 mmol) in 2-methoxyethanol (50 mL) at 130°C under an argon atmosphere for 16 h. After cooling to room temperature, the solvent was evaporated at low pressure. The obtained crude product was washed by water and then purified by column chromatography on silica gel using CH<sub>2</sub>Cl<sub>2</sub>/EtOAc as the eluent to afford a yellow product with a yield of 36% (0.75 g). <sup>1</sup>H NMR (400 MHz, DMSO-*d*<sub>6</sub>):  $\delta$  9.02 (1H, t), 8.25-8.19 (3H, m), 7.75-7.51 (14H, m), 6.97-6.90 (2H, m), 6.53 (1H, t), 6.32-6.30 (1H, m); <sup>31</sup>P NMR (162 MHz, DMSO-*d*<sub>6</sub>):  $\delta$  11.93; m/z: [M+1]<sup>+</sup> calc 655.1, found 654.8; Anal. Calcd for C<sub>30</sub>H<sub>22</sub>NO<sub>2</sub>PPt: C, 55.05; H, 3.39; N, 2.14; Found: C, 55.10; H, 3.36; N, 2.16.

**X-ray Crystallography.** Crystal diffraction data for Complexes Pt-1 and Ir-1 were measured on an Oxford Diffraction Xcalibur CCD diffractometer with graphite-monochromatized Mo-K $\alpha$  radiation ( $\lambda = 0.71073 \text{ \AA}$ ) at 291K using the  $\omega$ -scan technique. Programs CrysAlisPro was employed for data collection and data reduction.<sup>5</sup> The structures were solved by direct methods, and the non-hydrogen atoms were refined anisotropically by full-matrix least-squares method on F<sup>2</sup> using the SHELXTL-97 program.<sup>6</sup> Calculated hydrogen positions were input and refined in a riding manner along with the attached carbons. Complete crystal structure results of the complexes as CIF files including bond lengths, angles, and atomic coordinates are available as Supporting Information.

**Computational Methodology.** Calculations on electronic singlet and triplet states of the studied

complexes (Ir-1 and Pt-1) were carried out using the density functional theory (DFT) with the B3LYP hybrid functional.<sup>7</sup> Restricted and unrestricted formalisms were adopted in the singlet and triplet geometry optimization, respectively. TDDFT was used to calculate singlet and triplet excited state energies on the basis of the optimized structures. The basis set used for C, H, N, O and P atoms was 6-311G++(d, p) while effective core potentials with a LANL2DZ basis set was employed for the Ir or Pt atom. The solvent effect of CH<sub>2</sub>Cl<sub>2</sub> was taken into consideration using the integral equation formalism (IEF) version of the polarizable continuum model (PCM) with the dielectric constant of dichloromethane ( $\epsilon = 8.93$ ).<sup>8</sup> All computations described here were performed by using the Gaussian 09 package.<sup>9</sup>

**Device Fabrication and Characterization.** The OLED was fabricated by vacuum deposition of the materials at  $10^{-5}$  Pa onto ITO-coated glass substrates. Prior to the deposition of organic layers, the ITO surface was cleaned through ultrasonication sequentially with deionized water, methanol and acetone, followed by the treatment with UV-ozone. The organic layers were deposited thermally at a rate of 0.1 nm/s at the base pressure  $< 7 \times 10^{-5}$  Pa. Subsequently, LiF was deposited at 0.02 nm/s and then capped with Al (ca. 0.5 nm/s) by shadow masking without breaking the vacuum. Current-voltage-light intensity (*I-V-L*) and EL spectra were measured and recorded by using a Keithley 2000 digital multimeter and ST-900M spectrometer luminance meter.

## II. Characterization

**Table S1** Crystal data and details of data collection and refinement.

Compound reference	Pt-1	Ir-1
Chemical formula	C <sub>30</sub> H <sub>22</sub> NO <sub>2</sub> PPt•H <sub>2</sub> O	C <sub>41</sub> H <sub>30</sub> IrN <sub>2</sub> O <sub>2</sub> P•CH <sub>2</sub> Cl <sub>2</sub>
Formula Mass	672.56	890.77
Crystal system	triclinic	orthorhombic
<i>a</i> /Å	9.3743(4)	13.5063(4)
<i>b</i> /Å	11.2879(5)	18.2430(5)
<i>c</i> /Å	13.1326(5)	30.9506(15)
$\alpha$ /°	86.495(3)	90.00
$\beta$ /°	74.555(4)	90.00
$\gamma$ /°	74.730(4)	90.00
Unit cell volume/Å <sup>3</sup>	1292.10(9)	7626.1(5)
Temperature/K	291(2)	291(2)
Space group	<i>P</i> $\bar{1}$	<i>Pbca</i>
No. of formula units per unit cell, <i>Z</i>	2	8
Radiation type	Mo-K $\alpha$	Mo K $\alpha$
Absorption coefficient, $\mu$ /mm <sup>-1</sup>	5.524	3.721
No. of reflections measured	9692	20678
No. of independent reflections	5279	7796
<i>R</i> <sub>int</sub>	0.0355	0.0333
Final <i>R</i> <sub><i>I</i></sub> values ( <i>I</i> > 2 $\sigma$ ( <i>I</i> ))	0.0323	0.0451
Final <i>wR</i> ( <i>F</i> <sup>2</sup> ) values ( <i>I</i> > 2 $\sigma$ ( <i>I</i> ))	0.0600	0.1010
Final <i>R</i> <sub><i>I</i></sub> values (all data)	0.0397	0.0699
Final <i>wR</i> ( <i>F</i> <sup>2</sup> ) values (all data)	0.0638	0.1139
Goodness of fit on <i>F</i> <sup>2</sup>	1.021	1.042
CCDC number	969995	969996

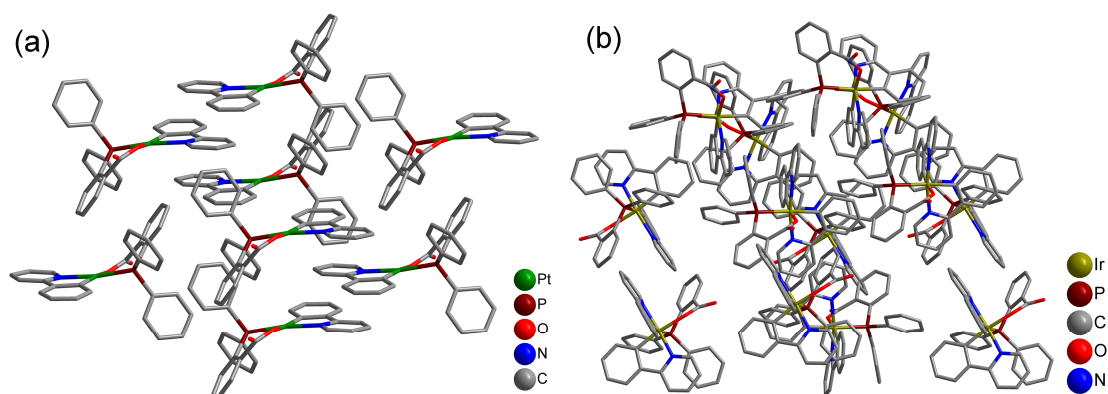


**Fig. S1** Crystal packing mode of Pt-1 (a) and Ir-1(b) complexes. Hydrogen atoms omitted for clarity.

**Table S2** Selected bond lengths (Å) and angles (deg) for Pt-1 and Ir-1 obtained from experimental data theory calculations in the gas as well as in CH<sub>2</sub>Cl<sub>2</sub>.

Distances (Å)	experiment	gas	CH <sub>2</sub> Cl <sub>2</sub>	Distances (Å)	experiment	gas	CH <sub>2</sub> Cl <sub>2</sub>
Pt(1)-C(1)	1.979(5)	2.01434	2.01234	Ir(1)-C(1)	2.053(6)	2.04643	2.04780
Pt(1)-N(1)	2.077(4)	2.09352	2.09875	Ir(1)-N(1)	2.075(5)	2.10339	2.10696
Pt(1)-O(1)	2.102(3)	2.12691	2.15560	Ir(1)-C(12)	2.002(7)	2.01676	2.01543
Pt(1)-P(1)	2.2097(12)	2.27625	2.28780	Ir(1)-N(2)	2.048(5)	2.06585	2.07065
				Ir(1)-O(1)	2.181(4)	2.20397	2.22481
				Ir(1)-P(1)	2.3701(16)	2.47480	2.47950
Angles (deg)	experiment	gas	CH <sub>2</sub> Cl <sub>2</sub>	Angles (deg)	experiment	gas	CH <sub>2</sub> Cl <sub>2</sub>
C(1)-Pt(1)-N(1)	80.22(18)	80.31235	80.24223	C(1)-Ir(1)-N(1)	79.6(2)	79.36296	79.38691
O(1)-Pt(1)-P(1)	87.37(10)	86.70384	86.38349	C(12)-Ir(1)-N(2)	80.5(3)	80.29543	80.24819
				O(1)-Ir(1)-P(1)	83.93(13)	78.39046	79.17219

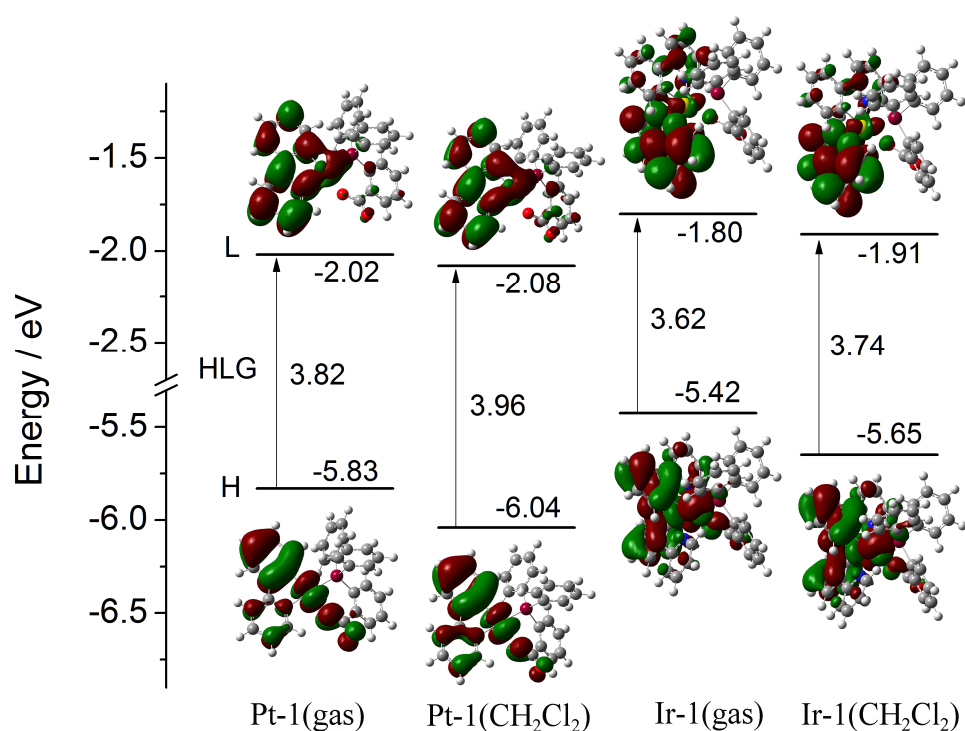


**Fig. S2** Molecular orbital diagram for the HOMOs/LUMOs and their energy levels of Pt-1 and Ir-1 calculated in the gas as well as in CH<sub>2</sub>Cl<sub>2</sub>

**Table S3** UV–vis absorption data of Pt-1 and Ir-1 in CH<sub>2</sub>Cl<sub>2</sub> ( $1.0 \times 10^{-5}$  mol/L) at 298 K versus that obtained from theory calculations.

Complex	Experimental (in CH <sub>2</sub> Cl <sub>2</sub> )		Theory (CH <sub>2</sub> Cl <sub>2</sub> )			
	$\lambda$ (nm)	$\epsilon$ ( $10^3 \text{ mol}^{-1} \text{ cm}^{-1}$ )	$\lambda$ (nm)	f	Character	Electronic transitions
Pt-1	384	4.73	386.9	0.0617	LLCT/MLCT	H-0→L+0(+98%)
	285	17.32	284.3	0.1817	ILCT/LLCT/MLCT	H-4→L+0(+55%) H-1→L+2(24%)
	229	39.78	245.0 244.0	0.1566 0.0595	ILCT/MLCT	H-0→L+8(+47%) H-4→L+2(+17%)
Ir-1	411	4.65	413.2	0.0382	LLCT/MLCT	H-0→L+0(+97%)
			399.6	0.0226		H-0→L+1(+97%)
	254	41.55	275.3	0.0804	ILCT/LLCT	H-0→L+9(+53%)
			269.2	0.1400		H-3→L+4(+39%)

Except for S<sub>1</sub> transitions, only calculated excitation with oscillator strength  $f \geq 0.05$  and singly excited configurations contributing more than 15% are listed.

**Table S4.** Compositions of the frontier molecular orbitals involved in the dominant UV–vis absorption based on the calculations in CH<sub>2</sub>Cl<sub>2</sub>.

Complex		H-4	H-1	H	L	L+2	L+8
Pt-1	Pt(%)	18.97	23.83	15.36	0.69	0.24	1.67
	ppy(%)	6.21	27.41	24.69	19.04	11.17	25.72
	HL1(%)	74.82	48.76	59.95	80.27	88.59	72.61
Complex		H-3	H	L	L+1	L+4	L+9
Ir-1	Ir(%)	4.70	11.23	0.43	1.04	2.54	0.90
	ppy(%)	45.36	31.08	64.51	77.56	36.28	34.30
	HL1(%)	49.94	57.69	35.06	21.40	61.18	64.80

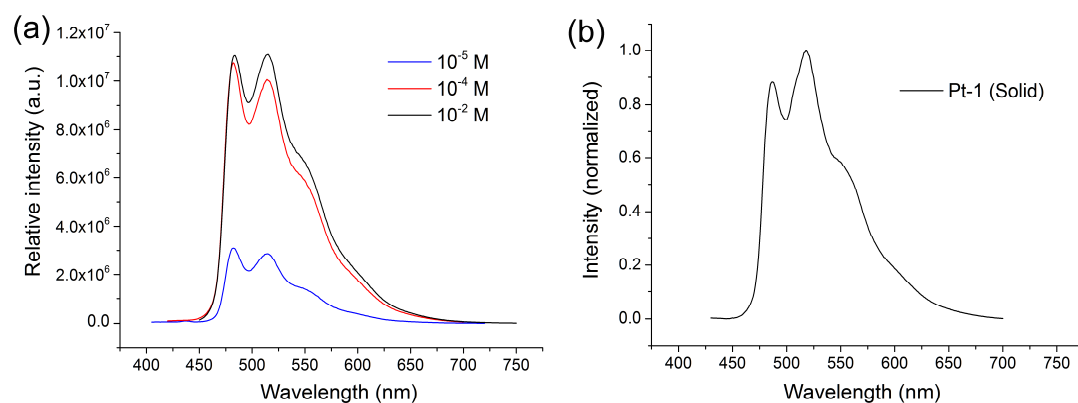


**Fig. S3** The photoluminescence of Pt-1 in CH<sub>2</sub>Cl<sub>2</sub> with concentrations from  $10^{-5}$  to  $10^{-2}$  M (a) and

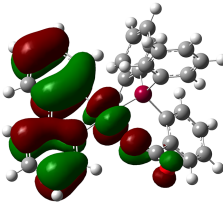
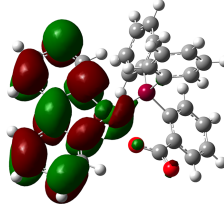
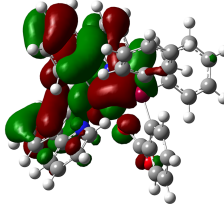
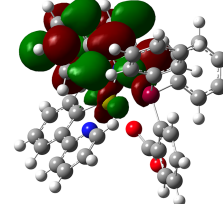
in solid-state (Powder) (b).

**Table S5.** Phosphorescence data of the Pt-1 and Ir-1 complexes and the calculated emission energies of  $T_1$  together with the composition of molecular orbital contributions.

	298K Solution		298K Solid (Powder)		Theory	
	$\lambda_{\max}$ (nm) / $\tau_{\text{obs}}$ ( $\mu\text{s}$ )	$\Phi$ (%) <sup>a</sup>	$\lambda_{\max}$ (nm)	$\Phi$ (%)	$\lambda_{\text{cal}}$ (nm)	Assignments
Pt-1	482, 516, 549 <sub>sh</sub> / 12.3	18.32	487, 518, 550 <sub>sh</sub>	23.30	593.25	HOMO $\rightarrow$ LUMO (88%)
Ir-1	502 / 1.1	0.91	--	--	562.06	HOMO $\rightarrow$ LUMO (83%)

<sup>a</sup> Phosphorescence quantum efficiency was measured in degassed  $\text{CH}_2\text{Cl}_2$  with  $\text{Ir}(\text{ppy})_3$  as the standard ( $\Phi = 0.40$ ).<sup>3</sup>

**Table S6.** Contributions of the frontier molecular orbitals of the complexes at the lowest triplet state ( $T_1$ ) based on calculations in  $\text{CH}_2\text{Cl}_2$ .

	HOMO	LUMO		HOMO	LUMO
Pt-1			Ir-1		
E/eV	-6.44	-3.65	E/eV	-6.02	-3.20
% contribution			% contribution		
Pt	16.20	1.01	Ir	9.08	0.98
ppy	77.90	92.10	ppy	30.49	64.58
HL1	5.90	6.89	HL1	60.43	34.44

**Table S7.** Selected bond lengths ( $\text{\AA}$ ) and angles (deg) for optimized Pt-1 and Ir-1 in  $T_1$  states based on calculations in  $\text{CH}_2\text{Cl}_2$ .

Pt-1	Distances ( $\text{\AA}$ )	Pt-1	Angles (deg)	Ir-1	Distances ( $\text{\AA}$ )	Ir-1	Angles (deg)
Pt(1)-C(1)	1.97050	C(1)-Pt(1)-N(1)	81.75829	Ir(1)-C(1)	2.03782	C(1)-Ir(1)-N(1)	79.70339
Pt(1)-N(1)	2.06962	O(1)-Pt(1)-P(1)	85.66454	Ir(1)-N(1)	2.11699	C(12)-Ir(1)-N(2)	82.14161
Pt(1)-O(1)	2.14735			Ir(1)-C(12)	1.97119	O(1)-Ir(1)-P(1)	75.90655
Pt(1)-P(1)	2.30917			Ir(1)-N(2)	2.06166		
				Ir(1)-O(1)	2.21477		

				Ir(1)-P(1)	2.54109		
--	--	--	--	------------	---------	--	--

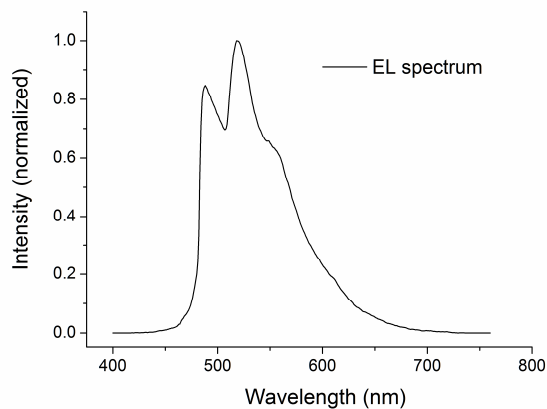


**Fig. S4** EL spectrum of the OLED based on Pt-1 as a phosphorescent dopant at 6 V.

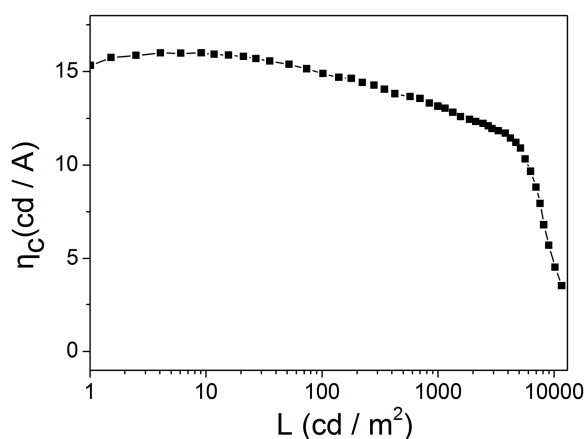


**Fig. S5** The current efficiency ( $\eta_c$ ) of the EL device versus luminance ( $L$ ).

Table S8. EL characteristics of the OLED using complex Pt-1 as a phosphorescent dopant.

	$V_{on}$ [V]	Max.B ( $cd\ m^{-2}$ )	$\eta_{ext}$ (%)	$\eta_p$ (lm/W)	$\eta_c$ (Cd/A)	CIE (x, y) at $100\ cd\ m^{-2}$
Pt-1	3.0	11651	4.93	14.64	15.99	(0.29, 0.58)

Abbreviations:  $\eta_{ext}$  = external quantum efficiency;  $\eta_p$  = power efficiency;  $V_{on}$  = turn-on voltage ( $1\ cdm^{-2}$ ); Max.B = maximum brightness at 12V.

### III. References:

- (a) E. Baranoff, B. F. E. Curchod, F. Monti, F. Steimer, G. Accorsi, I. Tavernelli, U. Rothlisberger, R. Scopelliti, M. Grätzel and M. K. Nazeeruddin, *Inorg. Chem.*, 2011, **51**, 799-811; (b) F. O. Garces, K. A. King and R. J. Watts, *Inorg. Chem.*, 1988, **27**, 3464-3471; (c) S. Sprouse, K. A. King, P. J. Spellane and R. J. Watts, *J. Am. Chem. Soc.*, 1984, **106**,



- 6647-6653; (d) K. Huang, H. Wu, M. Shi, F. Li, T. Yi and C. Huang, *Chem. Commun.*, 2009.
- (a) C. Li, S. Wang, Y. Huang, B. Zheng, Z. Tian, Y. Wen and F. Li, *Dalton Trans.*, 2013, **42**, 4059-4067; (b) J. Brooks, Y. Babayan, S. Lamansky, P. I. Djurovich, I. Tsyba, R. Bau and M. E. Thompson, *Inorg. Chem.*, 2002, **41**, 3055-3066.
  - (a) A. B. Tamayo, B. D. Alleyne, P. I. Djurovich, S. Lamansky, I. Tsyba, N. N. Ho, R. Bau and M. E. Thompson, *J. Am. Chem. Soc.*, 2003, **125**, 7377-7387; (b) Y. You and S. Y. Park, *J. Am. Chem. Soc.*, 2005, **127**, 12438-12439; (c) X. Yang, N. Sun, J. Dang, Z. Huang, C. Yao, X. Xu, C.-L. Ho, G. Zhou, D. Ma, X. Zhao and W.-Y. Wong, *Journal of Materials Chemistry C*, 2013, **1**, 3317-3326.
  - (a) D. P. Rillema, D. G. Taghdiri, D. S. Jones, L. A. Worl, T. J. Meyer, H. A. Levy and C. D. Keller, *Inorg. Chem.*, 1987, **26**, 578-585; (b) C. Shi, H. Sun, Q. Jiang, Q. Zhao, J. Wang, W. Huang and H. Yan, *Chem. Commun.*, 2013, **49**, 4746-4748; (c) X.-C. Hang, T. Fleetham, E. Turner, J. Brooks and J. Li, *Angew. Chem.*, 2013, **125**, 6885-6888.
  - Oxford Diffraction, Oxford Diffraction Ltd., Xcalibur CCD system, CrysAlis Software system, Version 1.171.34.39, 2010.
  - Sheldrick, G. M. SHELXL-97, *Program for the Refinement of Crystal Structures*; University of Göttingen: Göttingen, Germany, **1997**.
  - (a) E. Runge and E. K. U. Gross, *Phys Rev Lett*, 1984, **52**, 997-1000; (b) C. Lee, W. Yang and R. G. Parr, *Phys Rev B*, 1988, **37**, 785-789; (c) A. D. Becke, *The Journal of Chemical Physics*, 1993, **98**, 5648-5652.
  - (a) E. Cancès, B. Mennucci and J. Tomasi, *The Journal of Chemical Physics*, 1997, **107**, 3032-3041; (b) J. Tomasi, B. Mennucci and R. Cammi, *Chem Rev*, 2005, **105**, 2999-3094.
  - Frisch, M. J.; Trucks, G. W.; Schlegel, H. B.; Scuseria, G. E.; Robb, M. A.; Cheeseman, J. R.; Scalmani, G.; Barone, V.; Mennucci, B.; Petersson, G. A.; Nakatsuji, H.; Caricato, M.; Li, X.; Hratchian, H. P.; Izmaylov, A. F.; J. Bloino, G. Z.; Sonnenberg, J. L.; Hada, M.; Ehara, M.; Toyota, K.; Fukuda, R.; Hasegawa, J.; Ishida, M.; Nakajima, T.; Honda, Y.; Kitao, O.; Nakai, H.; Vreven, T.; Montgomery, J. A.; Jr.; Peralta, J. E.; Ogliaro, F.; Bearpark, M.; Heyd, J. J.; Brothers, E.; Kudin, K. N.; Staroverov, V. N.; Keith, T.; Kobayashi, R.; Normand, J.; Raghavachari, K.; Rendell, A.; Burant, J. C.; Iyengar, S. S.; Tomasi, J.; Cossi, M.; Rega, N.; Millam, J. M.; Klene, M.; Knox, J. E.; Cross, J. B.; Bakken, V.; Adamo, C.; Jaramillo, J.; Gomperts, R.; Stratmann, R. E.; Yazyev, O.; Austin, A. J.; Cammi, R.; Pomelli, C.; Ochterski, J. W.; Martin, R. L.; Morokuma, K.; Zakrzewski, V. G.; Voth, G. A.; Salvador, P.; Dannenberg, J. J.; Dapprich, S.; Daniels, A. D.; Farkas, O.; Foresman, J. B.; Ortiz, J. V.; Cioslowski, J.; Fox, D. J. *GAUSSIAN 09*, Revision C.01; Gaussian, Inc.: Wallingford, CT, **2010**.